Verification of WENO-type extrapolation with different WENO schemes

André C. Rialto[1], Luciano K. Araki[1], Nicholas D. P. da Silva[2], Rafael B. de R. Borges[3]

[1]*Dep. of Mechanical Engineering, Federal University of Paraná*
100 Coronel Francisco Heráclito dos Santos Avenue, 81530-900, Paraná, Brazil
rialtoandre@gmail.com, lucaraki@ufpr.br
[2]*Dep. of Mechanical Engineering, Maringá State University*
5790 Colombo Avenue, 87020-900, Paraná, Brazil
ndicati@gmail.com
[3]*Mathematics and Statistics Institute, Rio de Janeiro State University*
524 São Francisco Xavier Street, 20550-900, Rio de Janeiro, Brazil
rafael.borges@ime.uerj.br

Abstract. The usage of WENO-type extrapolation allows achieving high order and high resolution when solving fluid dynamics numerical problems with the finite difference method and rectangular meshes. Developing new modifications for this extrapolation implies better handling of boundary conditions. Hence, in this work, we are interested in the verification of three WENO-type extrapolations together with four WENO schemes in smooth and discontinuous test problems. Four different test problems modeled by the Euler equations will be solved with the finite difference method, positivity-preserving Lax-Friedrichs flux, and strong stability preserving Runge-Kutta. The first two are one-dimensional, and the others are two-dimensional. The one-dimensional discontinuous problem is a severe test case for the WENO-type extrapolations. The two-dimensional discontinuous problem is the double Mach reflection, which presents oblique shock and other nonlinear phenomena interacting with a wall. We show that the design accuracy is being reached for smooth problems, that the discontinuities and nonlinear phenomena are well captured, and we identify common features and areas of improvement for the WENO-type extrapolations.

Keywords: WENO-type extrapolation, CFD, high-resolution.

1 Introduction

In finite difference and volume methods, the properties at interfaces and boundaries are approximated values, as shown by Shu [1], and Tan and Shu [2]. Some nonlinear phenomena, such as shock waves, may appear inside the stencil used in the reconstruction, lowering the order and resolution of solution at boundaries. Many authors (Tan and Shu [3], Tan et al. [4], Lu et al. [5], Borges et al. [6], Lu et al. [7], Filbet and Yang [8]) have developed strategies to prevent or reduce this loss. One of them is the usage of WENO-type extrapolations, which allows to keep a high order and high resolution at the boundary in smooth problems. Alongside with this method, new types of WENO scheme can be used to better achieve the solution (Borges et al. [9], Acker, Borges, and Costa [10], van Lith, Thije Boonkkamp, and IJzerman [11], Zhu and Shu [12], Hong, Ye, and Ye [13]).

Adopting the strategy and smoothness indicators proposed by Wang, Shu, and Ning [4] and using improvements (Borges et al. [6], Lu et al. [7], Filbet and Yang [8]), we solved four CFD tests problems aiming the verification of WENO-type extrapolation with different WENO schemes.

2 Numerical methods

For this study, we are interested in the following set of equations

$$\boldsymbol{U}_t + \boldsymbol{F}(\boldsymbol{U})_x + \boldsymbol{G}(\boldsymbol{U})_y = \boldsymbol{0}\,, \tag{1}$$

with

$$\boldsymbol{U} = \begin{bmatrix} \rho \\ \rho u \\ \rho v \\ E \end{bmatrix}, \boldsymbol{F}(\boldsymbol{U}) = \begin{bmatrix} \rho u \\ \rho u^2 + p \\ \rho uv \\ u(E+p) \end{bmatrix}, \boldsymbol{G}(\boldsymbol{U}) = \begin{bmatrix} \rho v \\ \rho uv \\ \rho v^2 + p \\ v(E+p) \end{bmatrix}, \tag{2}$$

where ρ is the density, u and v are the x and y velocities, E is the total energy per unit volume, and p is the pressure.

We discretized the model equations with a Finite Difference conservative scheme (Shu [1])

$$\frac{d\boldsymbol{U}_{i,j}(t)}{dt} = -\frac{1}{\Delta x}\left(\widehat{\boldsymbol{F}}_{i+\frac{1}{2},j} - \widehat{\boldsymbol{F}}_{i-\frac{1}{2},j}\right) - \frac{1}{\Delta y}\left(\widehat{\boldsymbol{G}}_{i,j+\frac{1}{2}} - \widehat{\boldsymbol{G}}_{i,j-\frac{1}{2}}\right). \tag{3}$$

We also employed a positivity preserving Lax-Friedrichs flux splitting (Zhang and Shu [14])

$$\boldsymbol{F} \pm \left(\boldsymbol{U}_{i,j}\right) = \frac{1}{2}\left(\boldsymbol{U}_{i,j} \pm \frac{\boldsymbol{F}\left(\boldsymbol{U}_{i,j}\right)}{\alpha_x}\right), \tag{4}$$

where we use constant mesh sizes ($\Delta x = \Delta y$) and α_x is the maximum absolute eigenvalue for the entire domain.

We approximate the numerical flux with the Embedded WENO-JS and WENO-Z, multi-resolution, and WENO-Z+ schemes (Borges et al. [9], Acker, Borges and Costa [10], Lith, Boonkkamp, and IJzerman [11], Zhu and Shu [12]).

We employed the strong stability preserving Runge-Kutta to handle the time integration (Shu [1])

$$\begin{aligned} \boldsymbol{U}^{(1)} &= \boldsymbol{U}^n + \Delta t L(\boldsymbol{U}^n) \\ \boldsymbol{U}^{(2)} &= \frac{3}{4}\boldsymbol{U}^n + \frac{1}{4}\boldsymbol{U}^{(1)} + \frac{1}{4}\Delta t L\left(\boldsymbol{U}^{(1)}\right) \\ \boldsymbol{U}^{(n+1)} &= \frac{1}{3}\boldsymbol{U}^n + \frac{2}{3}\boldsymbol{U}^{(2)} + \frac{2}{3}\Delta t L\left(\boldsymbol{U}^{(2)}\right), \end{aligned} \tag{5}$$

where (1) is the first Runge-Kutta stage and (2) is the second, $L(\cdot)$ is the spatial approximation, n is the actual and $n+1$ is the next time step, and Δt is the time step.

The time steps were computed with the CFL number and (Lu et al. [5])

$$\Delta t = \min\left[\frac{CFL}{\alpha_x/\Delta x + \alpha_y/\Delta y}, \min(\Delta x, \Delta y)^{5/3}\right], \tag{6}$$

where α_y is the maximum absolute eigenvalue to the y-direction flux.

We imposed the boundary condition in only one boundary with known information and the WENO-type extrapolation of Tan et al. [4], Lu et al. [7], and Filbet and Yang [8]. At the other boundaries, we employed the analytical or exact solution, constant values, or periodic boundary conditions, depending on the problem at hand.

3 Test problems

3.1 One-dimensional Euler equations

Our first problem is a 1D smooth test case for the Euler equations. The domain and the initial condition were $[-\pi, \pi]$ and

$$\rho(x) = 1 + 0.2\sin(x)\,, \qquad u = 1, \qquad p = 2. \tag{7}$$

Then, the analytical solution is simply

$$\rho(x,t) = 1 + 0.2\sin(x - t)\,, \qquad u = 1, \qquad p = 2. \tag{8}$$

We used the analytical solution at the left boundary ghost points and focused on efforts at the right boundary. The velocity and pressure were constant and known at the boundary. For the density, we needed to compute the analytical solution for each Runge-Kutta step regarding (Tan et al. [4])

$$\begin{aligned} \rho^{n} &\sim \rho(t_n)\,, \\ \rho^{(1)} &\sim \rho(t_n) + \Delta t \frac{\partial \rho}{\partial t}(t_n)\,, \\ \rho^{(2)} &\sim \rho(t_n) + \frac{\Delta t}{2}\frac{\partial \rho}{\partial t}(t_n) + \frac{\Delta t^2}{4}\frac{\partial^2 \rho}{\partial t^2}(t_n)\,. \end{aligned} \tag{9}$$

Since $u = 1$, we have $\lambda_3 > \lambda_2 > 0$. Depending on the speed of sound magnitude ($\lambda_1 = u - a$), we imposed either one or no boundary conditions. If $\lambda_1 < 0$, we imposed one boundary condition. To do this, we used the ILW strategy, i.e., we computed ρ and $\partial\rho/\partial t$ with the analytical solution, extrapolated the second and third characteristic variables, and computed

$$V_1 = \frac{\rho - r_{21}V_2 - r_{31}V_3}{r_{11}}, \tag{10}$$

$$\frac{\partial V_1}{\partial x} = \frac{\partial \rho/\partial x - r_{21}(\partial V_2/\partial x) - r_{31}(\partial V_3/\partial x)}{r_{11}}. \tag{11}$$

Higher-order derivatives are available through the WENO-type extrapolation, as shown in Tan and Shu [2], Tan et al. [4], Lu et al. [7], Filbet and Yang [8]. With the characteristic variables and its derivatives at the boundary, we approximated the characteristic variables at the ghost points through a Taylor expansion

$$(V_m)_i = \sum_{k=0}^{4} \frac{(x_i - x_r)}{k!}\frac{\partial^k V_m}{\partial x^k}, \tag{12}$$

where x_r is the right boundary position. Then, at each ghost point

$$\boldsymbol{U}_i = \boldsymbol{R}\boldsymbol{V}_i\,. \tag{13}$$

For the smooth problem, we are interested in the accuracy results. As shown in Tab. 1, the WENO-Z+ with WENO-type extrapolation of Tan et al. [4] achieved the design order. We only show the accuracy results for this combination, since the other also achieved the design orders.

Table 1. L^1, L^2 and L^∞ norms and its orders for the 1D smooth problem density and $t_f = 1$.

Δx	L^1 norm	Order	L^2 norm	Order	L^∞ norm	Order
2π/10	3.05E – 03	-	6.23E – 03	-	1.91E – 02	-
2π/20	1.25E – 04	4.61	3.35E – 04	4.22	1.46E – 03	3.71
2π/40	1.42E – 06	6.46	2.23E – 06	7.23	1.10E – 05	7.05
2π/80	2.76E – 08	5.69	3.88E – 08	5.84	1.89E – 07	5.86
2π/160	7.29E – 10	5.24	9.76E – 10	5.31	4.53E – 09	5.38
2π/320	2.11E – 11	5.11	2.76E – 11	5.14	1.16E – 10	5.29

For the discontinuous problem, the domain and the initial condition were [-1,1] and

$$\rho(x) = \begin{cases} 0.4(x + 0.5) + 0.3, & -0.5 \le x \le 0, \\ 0.3, & \text{otherwise}, \end{cases} \tag{14}$$

$$u = 1, \qquad p = 2. \tag{15}$$

As long as the discontinuity remains in the domain, the analytical solution is

$$\rho(x,t) = \begin{cases} 0.4(x + 0.5 - t) + 0.3, & -0.5 \le x \le 0, \\ 0.3, & \text{otherwise}, \end{cases} \tag{16}$$

$$u = 1, \qquad p = 2\,, \tag{17}$$

where the final time is adjusted for each mesh. We left two points between the discontinuity and the end of the

domain. This represents a severe test case for the WENO-type extrapolations.

We also used the analytical solution at the left boundary ghost points and focused on efforts at the right boundary. For this problem, the properties are constant at the right boundary. Therefore,

$$\rho = 0.3, \qquad \frac{\partial \rho}{\partial x} = 0\,. \tag{18}$$

Since $\lambda_1 < 0$, we imposed one boundary condition with eq. (10) and eq. (11) and extrapolated the other characteristic variables with the WENO-type extrapolation. Then, we employed a Taylor expansion to compute the characteristic variable at the ghost points and transformed back to the conservative ones.

We show the density distribution in Figure 1 for the WENO-Z+ and WENO-type extrapolation of Tan et al. [4], where we can see good agreement between analytical and numerical solutions. We noticed that the WENO-MR and WENO-type extrapolation of Lu et al. [7] were most sensitive to the discontinuity. One can change the linear weights and other parameters to improve the convergence or reduce the sensitivity to the discontinuity.

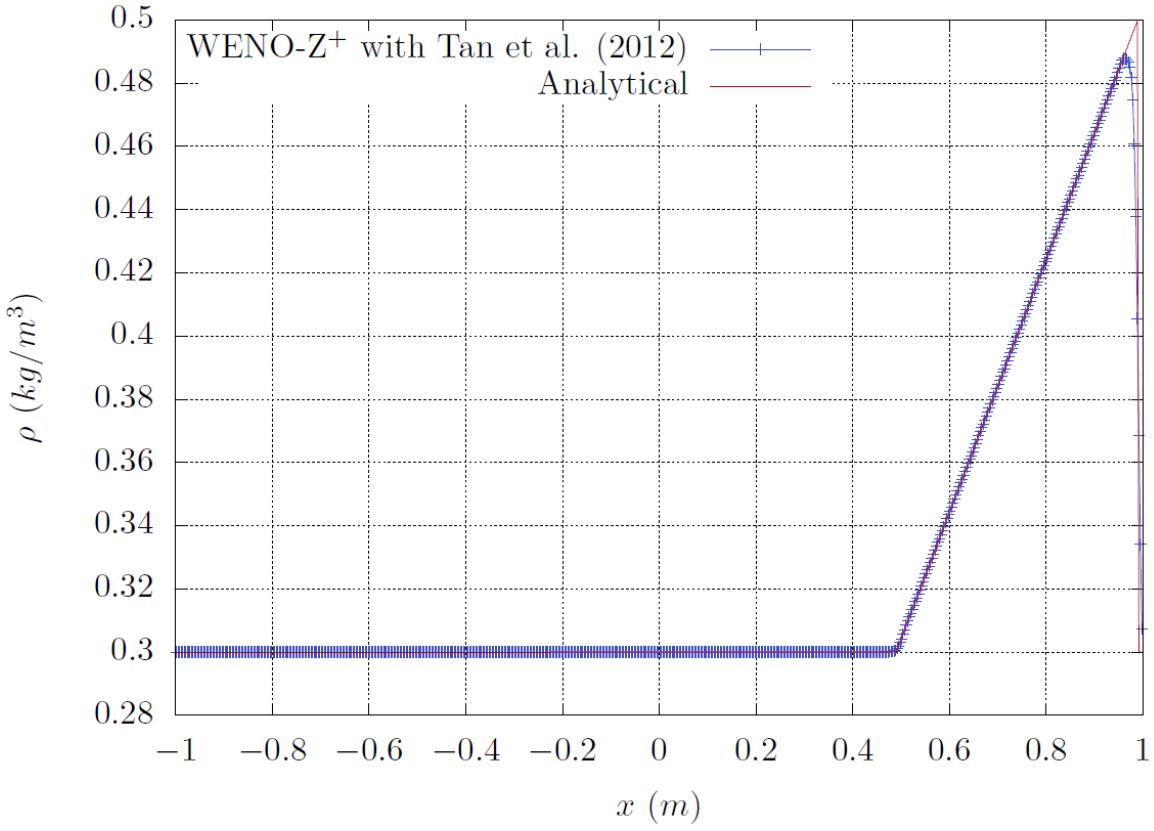

Figure 1. Density distribution for the discontinuous test problem with WENO-Z+, the WENO-type extrapolation of Tan et al. [4], and mesh with 640 points.

We remark that the WENO-type extrapolations have a dependency on the smaller stencil smoothness indicator. For Tan et al. [4] and Filbet and Yang [8] one have Δx^2, and for Lu et al. [7] a constant multiplied to smoothness indicator of the next stencil. The dependency on the mesh size causes trouble with the self similarity and the dependency on other stencils may present difficulties if the shock is too close to the boundary.

3.2 Two-dimensional Euler equations

Our first 2D problem is another smooth test case for the Euler equations. The domain and initial condition were [0,1] x [0,1] and

$$\rho(x,y) = 1 + 0.5\sin(2\pi x)\cos(2\pi y)\,, \qquad u = 1, \qquad v = -2, \qquad p = 2. \tag{19}$$

Then, the analytical solution is simply

$$\rho(x,y,t) = 1 + 0.5\sin[2\pi(x-t)]\cos[2\pi(y-t)], \qquad u = 1, \qquad v = -2, \qquad p = 2. \tag{20}$$

We employed the analytical solution at the upper boundary ghost points and periodic boundary conditions for left and right boundaries. By doing so, we focus on the WENO-type extrapolation at the lower boundary.

Since the *y*-velocity is negative and constant, we have an out flow at the lower boundary. $\lambda_{1,2,3} < 0$ and λ_4 may be positive or negative depending on the speed of sound. If $\lambda_4 = v + a > 0$ one should impose one boundary condition. Otherwise, none. We imposed the boundary conditions with the exact solution, ILW strategy, and the WENO-type extrapolation in a similar way as before, i.e., from eq. (9) to eq. (13).

We show the accuracy results in the Tab. 2 for the WENO-Z+ and WENO-type extrapolation of Tan et al. [4], where we can see that the design order was achieved. The other combinations between WENO and WENO-type extrapolation also achieved the design orders.

Table 2. L^1, L^2 and L^∞ norms and its orders for the 2D smooth problem density and $t_f = 1$.

Δx	L^1 norm	Order	L^2 norm	Order	L^∞ norm	Order
1/10	8.90E – 03	-	1.53E – 02	-	4.74E – 02	-
1/20	8.18E – 04	3.44	2.00E – 03	2.93	8.69E – 03	2.45
1/40	2.96E – 05	4.79	1.26E – 04	3.99	1.11E – 03	2.97
1/80	1.75E – 07	7.40	2.50E – 07	8.97	1.05E – 06	10.0
1/160	5.39E – 09	5.02	7.68E – 09	5.02	3.49E – 08	4.91

Our last test case is the double Mach reflection, where an inclined oblique shock is sent to a horizontal wall. This is an interesting test case because of the interaction between nonlinear phenomena and the wall. The domain and initial condition were $[0,4]\ x\ [0,1]$ and

$$(\rho,u,v,p) = \begin{cases} (8, 4.125\sqrt{3}, -4.125, 116.5), & x < \dfrac{1}{6} + \dfrac{y}{\sqrt{3}}, \\ (1.4, 0, 0, 2.5), & \text{otherwise.} \end{cases} \tag{21}$$

For this problem, we know the shock position at the upper boundary

$$s(t) = \frac{1}{6} + \frac{(1+20t)}{\sqrt{3}}. \tag{22}$$

Therefore, we imposed constant values at the upper boundary regarding the shock position

$$(\rho,u,v,p) = \begin{cases} (8, 4.125\sqrt{3}, -4.125, 116.5), & x < s(t), \\ (1.4, 0, 0, 2.5), & \text{otherwise.} \end{cases} \tag{23}$$

At the left boundary we imposed constant values to the left of the shock and at the right boundary we employed a lower-order extrapolation. Then, we can concentrate in testing the WENO-type extrapolation at the lower boundary wall. We choose this boundary because the nonlinear phenomena interacted with it during the simulation.

Since $v = 0$ at the wall, we have $\lambda_1 = v - a < 0$, $\lambda_{2,3} \approx 0$, and $\lambda_4 = v + a > 0$. That is, we need to impose one boundary condition (Lu et al. [7])

$$V_4 = \frac{-r_{31}V_1 - r_{32}V_2 - r_{33}V_3}{r_{34}}, \tag{24}$$

$$\frac{\partial V_4}{\partial y} = \frac{-r_{31}(v-a)(\partial V_1/\partial y) - r_{32}v(\partial V_2/\partial y) - r_{33}v(\partial V_3/\partial y)}{r_{34}(v+a)}. \tag{25}$$

The other derivatives are available through the WENO-type extrapolation. We again employed a Taylor expansion to compute the ghost points. Then, changed back to the conservative variables.

We show the density color map and contours from 1 to 23 for the WENO-Z+ and WENO-type extrapolation of Tan et al. [4] in Fig. 2, where we can see that the shock and non-linear phenomena were well captured. Other combinations also presented a good representation of flow features. Exception is made for the WENO-type

extrapolation of Filbet and Yang [8] that was most sensitive to the shock.

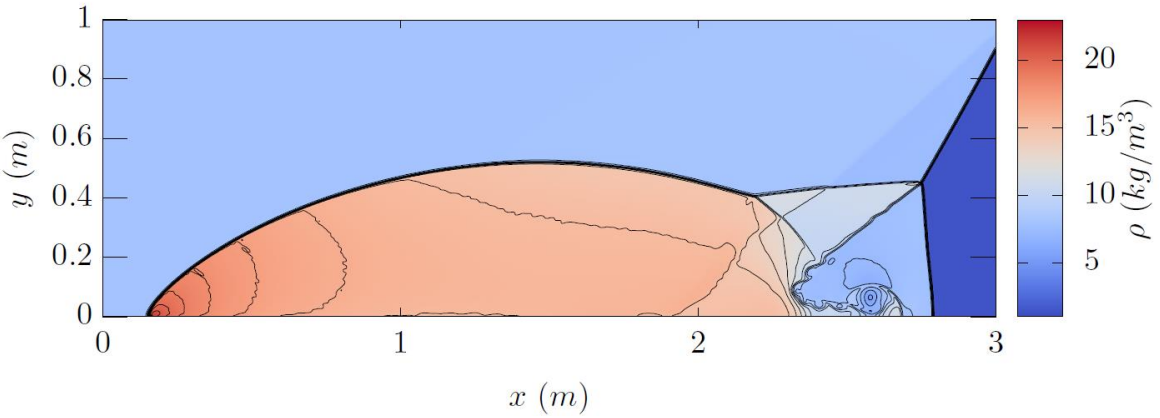

Figure 2. Density color map and contours for the double Mach reflection with WENO-Z+, the WENO-type extrapolation of Tan et al. [4], and mesh with 1200 x 300 points.

4 Conclusions

Test problems of high order and resolution at boundaries were verified using WENO-type extrapolation combined with four different WENO schemes: WENO embedded Z, WENO embedded JS, WENO-MR and WENO-Z+.

For the first test, a 1D smooth Euler equation, our results showed that all four combinations were able to achieve the desired accuracy. On the second test, 1D Euler equation with discontinuities, the WENO-Z+ and WENO-type extrapolation of Tan et al. [4] had a good agreement between analytical and numerical solutions. In this particular case, we observed that the WENO-MR with WENO-type extrapolation of Lu et al. [7] were more sensitive to discontinuities than the others. The results of the third test, a 2D smooth Euler equation, proved that the combinations we employed were accurate. As for the last test, 2D Euler equation with discontinuities, we were able to acquire desired results in capturing the non-linear phenomena and flow features, with the exception of the WENO-type extrapolation of Filbet and Yang [8], that was most sensitive to the shock in this case. Although we did not test, the WENO-type parameters can be changed to improve the convergence.

Overall, we show the design accuracy is being reached for smooth problems, and that the discontinuities and nonlinear phenomena are well captured for new WENO-type schemes, ensuring high order and resolution at boundaries. We also identified that one can improve the WENO-type extrapolations by reducing or eliminating the dependency of nonlinear weights on smaller stencils.

Authorship statement. The authors hereby confirm that they are the sole liable persons responsible for the authorship of this work, and that all material that has been herein included as part of the present paper is either the property (and authorship) of the authors, or has the permission of the owners to be included here.

References

[1] C.-W. Shu. “Essentially non-oscillatory and weighted essentially non-oscillatory schemes for hyperbolic conservation laws”, pp. 325-432. *Springer Berlin Heidel-berg*, Berlin, Heidelberg, 1998.
[2] S. Tan and C.-W. Shu. “Inverse Lax-Wendroff procedure for numerical boundary conditions of conservation laws”. *Journal of Computational Physics*, vol. 229, n. 21, pp. 8144-8166, 2010.
[3] S. Tan and C.-W. Shu. “A high order moving boundary treatment for compressible inviscid flows”. *Journal of Computational Physics*, vol. 230, n. 15, pp. 6023-6036, 2011.
[4] S. Tan, C. Wang, C.-W. Shu, and J. Ning. “Efficient implementation of high order inverse Lax-Wendroff boundary treatment for conservation laws”. *Journal of Computational Physics*, vol. 231, n. 6, pp. 2510-2527, 2012.
[5] J. Lu, J. Fang, S. Tan, C.-W. Shu, and M. Zhang. “Inverse Lax-Wendroff procedure for numerical boundary conditions of convection-diffusion equations”. *Journal of Computational Physics*, vol. 317, pp. 276-300, 2016.

[6] R. B. de R. Borges, N. D. P. da Silva, F. A. A. Gomes, C.-W. Shu, and S. Tan. "A sequel of inverse Lax-Wendroff high order wall boundary treatment for conservation laws". *Archives of Computational Methods in Engineering*, July 2020.
[7] J. Lu, C.-W. Shu, S. Tan, and M. Zhang. "An inverse Lax-Wendroff procedure for hyperbolic conservation laws with changing wind direction on the boundary". *Journal of Computational Physics*, vol. 426, pp. 109940, 2020.
[8] F. Filbet and C. Yang. "An inverse Lax-Wendroff method for boundary conditions applied to Boltzmann type models". *Journal of Computational Physics*, vol. 245, pp. 43-61, 2013.
[9] R. Borges, M. Carmona, B. Costa, and W. S. Don. "An improved weighted essentially non-oscillatory scheme for hyperbolic conservation laws". *Journal of Computational Physics*, vol. 227, n. 6, pp. 3191-3211, 2008.
[10] F. Acker, R. B. de R. Borges, and B. Costa. "An improved WENO-Z scheme". *Journal of Computational Physics*, vol. 313, pp. 726-753, 2016.
[11] B. S. van Lith, J. H. ten Thije Boonkkamp, and W. L. IJzerman. "Embedded WENO: A design strategy to improve existing WENO schemes". *Journal of Computational Physics*, vol. 330, pp. 529-549, 2017.
[12] J. Zhu and C.-W. Shu. "A new type of multi-resolution WENO schemes with increasingly higher order of accuracy". *Journal of Computational Physics*, vol. 375, pp. 659-683, 2018.
[13] Z. Hong, Z. Ye, and K. Ye. "An improved WENO-Z scheme with symmetry-preserving mapping". *Advances in Aerodynamics*, vol. 2, n. 1, p. 18, Aug. 2020.
[14] X. Zhang and C.-W. Shu. "Positivity-preserving high order finite difference WENO schemes for compressible Euler equations". *Journal of Computational Physics*, vol. 231, n. 5, pp. 2245-2258, 2012.